

## The Lamellar Structure of Certain Microcline and Anorthoclase

BY T. ITO AND R. SADANAGA

*Mineralogical Institute, University of Tokyo, Hongo, Tokyo, Japan*

(Received 8 August 1951 and in revised form 16 November 1951)

The interlamination on a microscopic to submicroscopic scale of different feldspars in microcline and anorthoclase has been studied using Weissenberg photographs ( $\text{Co } K\alpha$ ,  $\lambda = 1.79 \text{ \AA}$ ) and the results have been correlated with those of chemical analysis. They are all composed of two or more discrete member-crystals, one being monoclinic or triclinic and potash-rich, and the remainder triclinic and soda-rich. The constants of the direct and reciprocal lattices of each component feldspar are given. Soda feldspars are either albite- or pericline-twinned according as the  $\gamma^*$  or  $\gamma$  angle of the reciprocal or direct lattice is  $90^\circ$ . Further, the possible relationship between the bulk composition of a feldspar belonging to the potash-soda series and twinning of the soda feldspars produced from it upon exsolution has been surmised. The triclinic symmetry of the potash component of microcline has been confirmed.

The possible interlamination on a submicroscopic scale of two different crystals in certain feldspars first emerged in the works of Kôzu (Kôzu & Endô, 1921; Kôzu & Suzuki, 1921) and of Hadding (1921). The characteristic doubling of Laue spots, which vanishes on heating and reappears on cooling, demonstrated strikingly that these feldspars, though apparently uniform to the naked eye or under the microscope, are actually split into two member-crystals in a definite mutual orientation. Later, one of the present writers (Ito, 1938), studying the same moonstone specimens on which Kôzu experimented, found that there exists in it a monoclinic soda feldspar, along with a potash feldspar. Chao & Taylor (1940), however, interpreted their experimental results, as well as ours, as due to the presence of a triclinic twinned, and not of a monoclinic, soda feldspar. That we were looking only on one side of things has been shown by our recent re-examination of moonstone (Ito, 1950, p. 122), which revealed that it is of an unusually complex nature and is composed of two monoclinic and two or more triclinic feldspars, the latter, as Taylor pointed out, being invariably twinned. We give below an account of further examples of feldspars which, though less complex, are similarly constituted.

### 1. Procedure of analysis

We have adopted here the same method as in our above-mentioned study of moonstone. Since the course of analysis in its experimental and theoretical implications has already been discussed and described in detail, we may assume it to be generally known and will now sketch it only briefly.

In the first place, we took rotation photographs ( $\text{Co } K\alpha$ ,  $\lambda = 1.79 \text{ \AA}$ ) about each of the crystallographic axes or about the directions simply related thereto, obtaining patterns as simple as possible. The object of these experiments was to find a direction or

directions common to the constituent crystals that make up the feldspar examined. The rotation photograph about such a direction will be very simple and lend itself to easy indexing. When twinning was suspected to exist in any of the component crystals, search was further made for the possible twin axis or plane. The rotation photograph of a twin about its twin axis has an appearance similar to that of a single crystal, with all the spots lying perfectly on the layer lines, whereas a slight deviation of the rotation axis from twin axis will distort considerably the regular alignment of spots in the photograph. In cases where a twin plane was in question, one of the zone axes belonging to it was chosen as the rotation axis, for they are the directions left unchanged (except for their sense) by the twinning operation.

These preliminary surveys of the rotation photographs have determined the course of our further experiments, indicating the directions about which the Weissenberg photographs should profitably be taken. The Weissenberg photographs in Buerger's (equi-inclination) version ( $\text{Co } K\alpha$ ,  $\lambda = 1.79 \text{ \AA}$ ; camera radius 3.41 cm.; film movement coupled with the rotating crystal  $1^\circ$  to 1 mm.) have furnished us with data on the reciprocal lattices, layer by layer, of the composite crystal. Piling up, as prescribed by experiment, the reciprocal net-planes thus derived we reconstructed the composite lattice representative of the nature of the interpenetrating crystals. Thereupon the constants of (direct) lattices were calculated (Buerger, 1937), and the laws and mode of twinning and intergrowth of the component crystals were deduced.

The relative intensity of reflexions in the Weissenberg photographs has been utilized to estimate the amount of each component feldspar on the assumption that they are structurally of the same type as those worked out by Taylor. Intensities were measured for the most part visually, following the multiple photo-

graphic technique (Lange, Robertson & Woodward, 1939) and taking into account the definite intensity ratio of  $\alpha$  to  $\beta$  radiation (7:1). Ratios were obtained by comparing the reflexions with the same ( $hkl$ ), due regard having always been paid to splitting or overlapping of spots to be ascribed either to twinning or parallel growth, coupled by the contingent identity of certain constants. These ratios were then converted for each  $hkl$ , taking into account the theoretical  $F$  values based on the structures of Taylor, to the ratios expressing the relative amount of the component feldspars. Ordinarily 30–40 pairs or trios (sometimes quartets or quintets) of reflexions were used to obtain the final ratio.

## 2. Microcline

The microcline examined is from the Paotze (Hoshi) mica mine, near Shongchin, Hamkvong, North Korea (Ito, 1935, p. 179). It is over  $40 \times 30 \times 10$  cm. in size and is of conspicuously triclinic habit with (010), (110), ( $1\bar{1}0$ ), (001), (130), ( $201$ ), (021) and ( $1\bar{1}1$ ) well developed. The typical microcline structure is visible under the microscope. The result of chemical analysis carried out on material picked up under the polarizing microscope and free from inclusions or decay substances is given in Table 1.

We give in Fig. 1 the Weissenberg diagrams of microcline and the reciprocal net planes corresponding to them, together with the reciprocal unit cells reconstructed. They illustrate the way in which microcline is resolved into component feldspars. In Fig. 1(a) rotation is about the  $a$  axis of one of the two components and is parallel to the (001)–(010) edge of the (macroscopic) crystal. The zero layer was photo-

graphed. This shows that one component feldspar is definitely triclinic and untwinned while the partner, also triclinic, is albite-twinned with  $[001]^*$  of the latter visibly branching out into double lines. It is to be noted that  $(b^*c^*)_0$  net planes of these two intergrown feldspars are not strictly on the same plane, but the reflexions arising from them are observed on the same  $a(0)$ -photograph taken, as above mentioned, setting up the specimen with reference to one of its components, owing to the tolerably finite width of the slit used.

The  $c(0)$ -diagram (Fig. 1(b)) indicates that  $(a^*b^*)_0$  net planes of both feldspars are perfectly on the same level. The reciprocal-lattice lines are simple everywhere on this level. On the higher levels, however, we notice that one set of spots representing one of the component feldspars are all split into doublets, showing that albit twinning has come into play. On  $(a^*b^*)_1$  level for example (Fig. 1(c))  $[100]^*$  lines are all doubled whereas  $[010]^*$  lines remain simple.

In Table 2(a) are given the constants of the direct and reciprocal lattices of the component feldspars determined. We may deduce from these and from the interpretation of the Weissenberg diagrams, as given above, that the microcline examined consists of two discrete constituents grown side by side. Both of them are triclinic in symmetry but, on the basis of their respective lattice constants, one should be potash-rich and the other soda-rich. The potash feldspar is free from twinning and the soda feldspar twinned after the albite law. They are associated in such a way that (100) and  $[001]$  of one are respectively parallel to those of the other. This can take place only when the  $\gamma^*$  angle of the twinned feldspar is, as in the present case, just  $90^\circ$ , for, whereas albite twinning leaves  $[001]$  unaltered in orientation, it brings (100) generally in the juxtaposed, and not in the parallel, positions.

Thanks to the coexistence in parallel growth of the triclinic twinned (soda) feldspar, the triclinic nature of the untwinned (potash) feldspar has been brought to light without ambiguity, the uncertainty as to the obliqueness, if not the possible inaccuracy of the absolute values, of the axial angles having been automatically eliminated by the geometry of the reciprocal lattice as revealed on the Weissenberg diagrams. The axial angles of microcline determined by us agree qualitatively with those obtained goniometrically by Böggild (1911) many years ago, and with those obtained recently by Laves (1950) using an X-ray precession camera.

From the intensities of X-ray reflexions measured in the Weissenberg photographs it has been estimated that the microcline contains 82% potash feldspar and 18% soda feldspar, roughly in conformity with the ratio 77:23 of the potash to soda components as calculated from chemical analysis. The agreement is satisfactory inasmuch as we have simply discarded the possible isomorphous replacement of the soda and potash as well as lime contents.

Table 1. *Chemical composition of the potash-soda feldspars studied*

	(1)	(2)	(3)
SiO <sub>2</sub>	62.88 %	65.39 %	60.33 %
Al <sub>2</sub> O <sub>3</sub>	19.79	19.78	20.70
Fe <sub>2</sub> O <sub>3</sub>	1.39	0.70	2.60
FeO	—	0.05	0.03
MnO	None	—	—
MgO	0.18	0.48	0.69
CaO	0.43	0.67	0.84
K <sub>2</sub> O	11.98	9.46	7.96
Na <sub>2</sub> O	2.42	2.16	5.34
H <sub>2</sub> O(+)	0.37	0.62	0.66
H <sub>2</sub> O(—)	0.43	0.39	0.71
Total	99.87	99.70	99.86
KAISi <sub>3</sub> O <sub>8</sub>	74.7	71.2	47.4
NaAlSi <sub>3</sub> O <sub>8</sub>	22.9	24.6	48.4
CaAl <sub>2</sub> Si <sub>2</sub> O <sub>8</sub>	2.4	4.2	4.2
Or : Ab	77 : 23	74 : 26	49 : 51

(1) Microcline from the Paotze (Hoshi) mica mine, North Korea. Analysis by H. Minato, 1951.

(2), (3) Anorthoclase from Minchon (Meisen), North Korea. Analysis by H. Kaneko, 1951. (2) Rim part. (3) Core part.

Table 2. *Lattice constants of the potash-soda feldspars*

(a) Microcline from Paotze, N. Korea			
	I'. K-rich, triclinic†	II'. Na-rich, triclinic††	
$a^*$ (Å <sup>-1</sup> )	0.129 <sub>5</sub>	0.137 <sub>2</sub>	
$b^*$ (Å <sup>-1</sup> )	0.076 <sub>5</sub>	0.077 <sub>5</sub>	
$c^*$ (Å <sup>-1</sup> )	0.152 <sub>7</sub>	0.156 <sub>0</sub>	
$\alpha^*$	90° 18' ± 6'	87° 06' ± 10'	
$\beta^*$	63° 42' ± 6'	64° 02' ± 10'	
$\gamma^*$	89° 24' ± 6'	90° 00' ± 6'	
$a$ (Å)	8.61 ± 0.02	8.11	
$b$ (Å)	13.06 ± 0.03	12.92	
$c$ (Å)	7.30 ± 0.01	7.14 ± 0.04	
$\alpha$	89° 22'	93° 14'	
$\beta$	116° 18'	116° 01'	
$\gamma$	90° 50'	88° 35'	
(b) Anorthoclase from Chilposan, N. Korea			
	I''. K-rich, monoclinic	II''. Na-rich, triclinic††	III''. Na-rich, triclinic§
$a^*$ (Å <sup>-1</sup> )	0.131 ± 0.001	0.137 ± 0.001	0.137 ± 0.001
$b^*$ (Å <sup>-1</sup> )	0.077 ± 0.002	0.077 ± 0.001	0.077
$c^*$ (Å <sup>-1</sup> )	0.155 ± 0.002	0.155	0.155 ± 0.001
$\alpha^*$	—	88° 10' ± 10'	88° 10' ± 10'
$\beta^*$	63° 30' ± 6'	64° 00' ± 10'	63° 48' ± 6'
$\gamma^*$	—	90° 00' ± 6'	89° 15' ± 10'
$a$ (Å)	8.53 ± 0.03	8.12	8.14
$b$ (Å)	13.0 ± 0.05	13.0	13.0 ± 0.05
$c$ (Å)	7.21 ± 0.03	7.18 ± 0.04	7.19
$\alpha$	—	92° 08'	91° 40'
$\beta$	116° 30'	116° 00'	116° 10'
$\gamma$	—	89° 10'	90° 00'

† Determined directly:  $a^*$ ,  $b^*$ ,  $c^*$ ,  $\alpha^*$ ,  $\beta^*$ ,  $\gamma^*$ ,  $a$ ,  $b$ ,  $c$ ; derived by calculation:  $\alpha$ ,  $\beta$ ,  $\gamma$ .

†† Determined directly:  $a^*$ ,  $b^*$ ,  $\gamma^*$ ,  $c$ ; determined by the method of 'dome-offset' (Buerger, 1937):  $\alpha^*$ ,  $\beta^*$ ; derived by calculation:  $c^*$ ,  $a$ ,  $b$ ,  $\alpha$ ,  $\beta$ ,  $\gamma$ .

§ Determined directly:  $a^*$ ,  $c^*$ ,  $\beta^*$ ,  $b$ ; determined by the method of 'dome-offset':  $\alpha^*$ ,  $\gamma^*$ ; derived by calculation:  $b^*$ ,  $a$ ,  $c$ ,  $\alpha$ ,  $\beta$ ,  $\gamma$ .

(c) Moonstone from Minchon, N. Korea (Ito, 1950, p. 129)

	I'''. K-rich, monoclinic	II'''. Na-rich, monoclinic	III'''. Na-rich, triclinic	IV'''. Na-rich, triclinic	V'''. Na-rich, triclinic
$a^*$ (Å <sup>-1</sup> )	0.130 <sub>0</sub>	0.137 <sub>0</sub>	0.137 <sub>0</sub>	0.137 <sub>0</sub>	0.137 <sub>0</sub>
$b^*$ (Å <sup>-1</sup> )	0.077 <sub>3</sub>	0.077 <sub>3</sub>	0.077 <sub>3</sub>	0.077 <sub>3</sub>	0.077 <sub>3</sub>
$c^*$ (Å <sup>-1</sup> )	0.156 <sub>2</sub>	0.156 <sub>2</sub>	0.156 <sub>2</sub>	0.156 <sub>2</sub>	0.156 <sub>2</sub>
$\alpha^*$	—	—	88° 18'	87° 22'	86° 27'
$\beta^*$	63° 40'	63° 50'	63° 50'	63° 50'	63° 50'
$\gamma^*$	—	—	89° 15'	88° 50'	88° 28'
$a$ (Å)	8.58 <sub>2</sub>	8.13 <sub>5</sub>	8.13 <sub>4</sub>	8.13 <sub>5</sub>	8.13 <sub>5</sub>
$b$ (Å)	12.94 <sub>0</sub>	12.94 <sub>0</sub>	12.94 <sub>5</sub>	12.95 <sub>3</sub>	12.96 <sub>5</sub>
$c$ (Å)	7.14 <sub>4</sub>	7.13 <sub>4</sub>	7.13 <sub>3</sub>	7.14 <sub>0</sub>	7.14 <sub>5</sub>
$\alpha$	—	—	91° 31'	92° 22'	93° 13'
$\beta$	116° 20'	116° 10'	116° 09'	116° 09'	116° 08'
$\gamma$	—	—	90° 00'	90° 00'	90° 00'

### 3. Anorthoclase

The anorthoclase crystals examined came from Chilposan (Shichi-hō-san), near Minchon, Hamkvong, North Korea and are the same as described morphologically in detail by N. Katayama (Ito, 1935, p. 172). Crystals are rather rarely single, being mostly twins (macroscopic) after complicated laws. Dimensions were up to several centimetres. The individuals that make up these aggregates are usually built in tones, the outermost layer showing schillerization like

moonstone, but very faint, and the core containing minute inclusions, mostly pyroxenes and olivines. This anorthoclase occurs, accompanied sometimes by moonstone, in certain alkaline trachyte which is developed extensively in the district.

After having thoroughly sorted out the specimens under the polarizing microscope, chemical analyses were carried out separately on the samples taken from the rim and core of a crystal, with the results given in Table 1.

Weissenberg photographs were taken of the slips

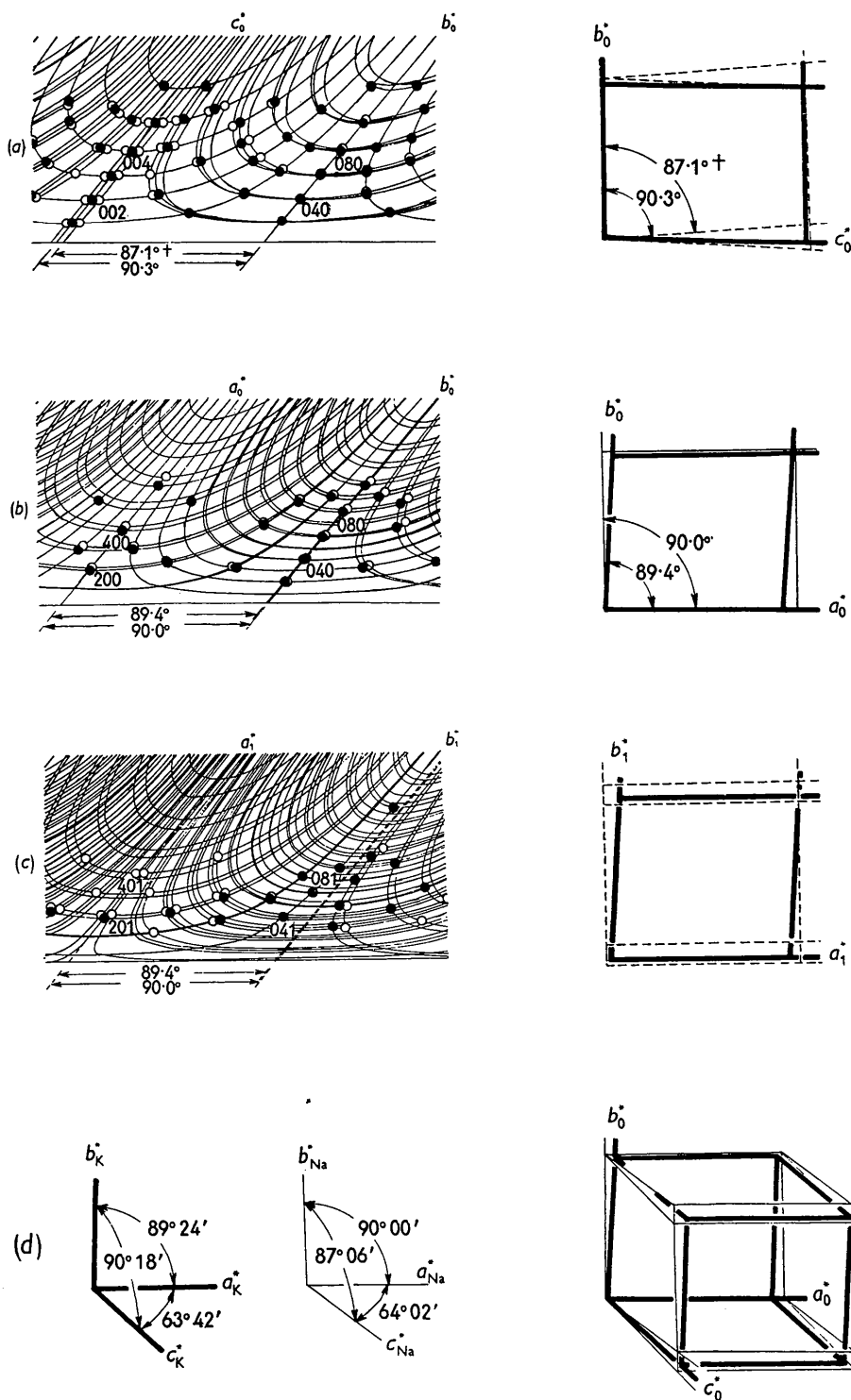


Fig. 1. Weissenberg diagrams of microcline, showing that it is composed of two triclinic crystals, one being untwinned potassium felspar and the other albite-twinned sodium felspar. The accompanying figures give the reciprocal-net planes derived from, and corresponding to, them. Black circles represent potassium felspar, open circles sodium felspar. Thick lines represent lattice lines of potassium felspar and thin lines those of sodium felspar. Broken lines indicate that the net plane is not on the same plane with the other associated. (a) Rotation about the  $a$  axis of potassium-felspar; zero layer. (b) Rotation about the  $c$  axis of potassium and sodium felspars which are parallel to each other; zero layer. (c) Rotation the same as (b); first layer. (d) The composite reciprocal lattice reconstructed. ( $\dagger$  indicates that the angle is measurable only approximately on this diagram.)

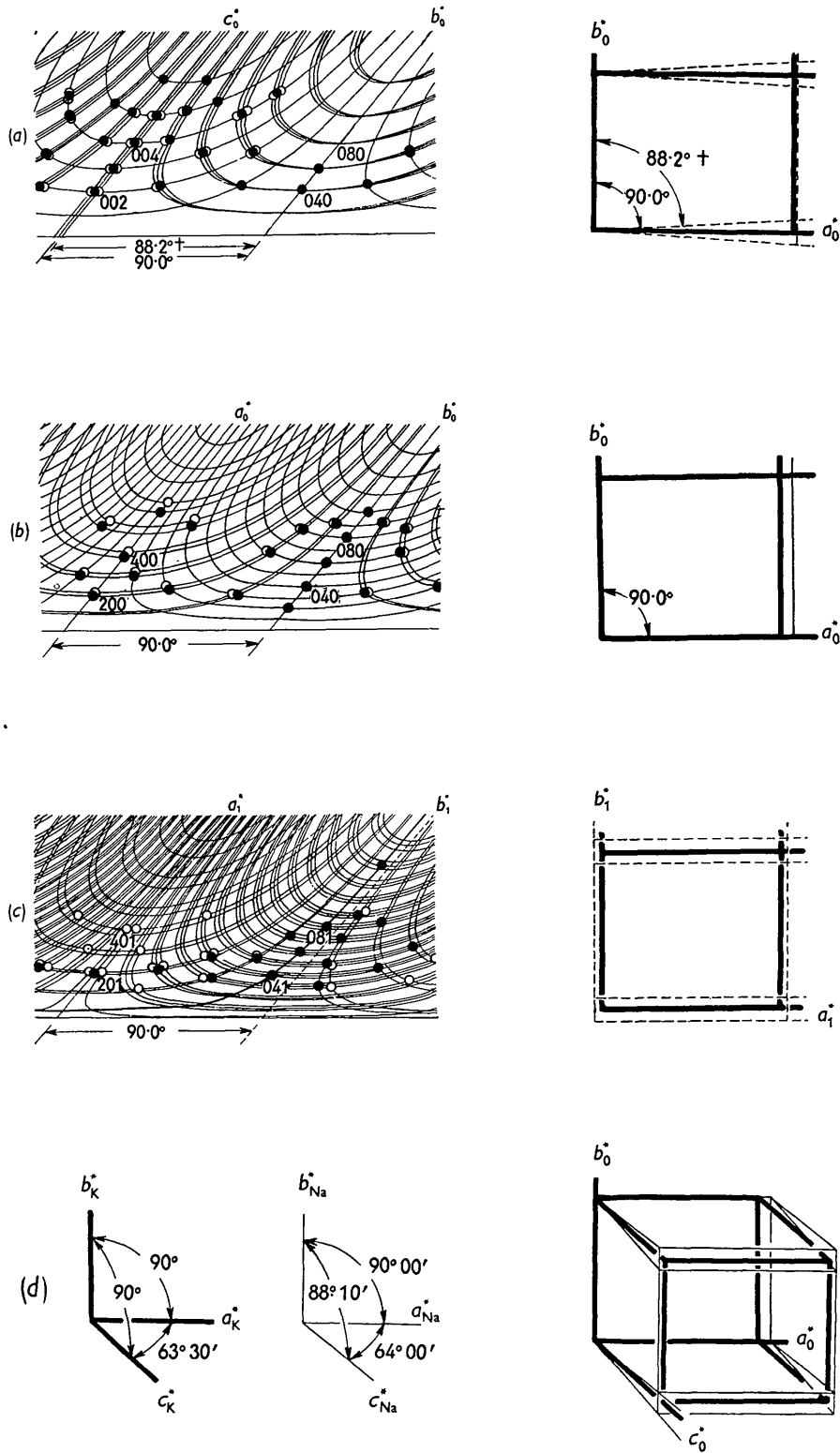


Fig. 2. Weissenberg diagrams of anorthoclase (rim part), showing that it is composed of two crystals, one being monoclinic potassium feldspar and the other triclinic and albite-twinned sodium feldspar. Notation as in Fig. 1. (a) Rotation about the *a* (monoclinic) axis; zero layer. (b) Rotation about the *c* (monoclinic and triclinic)-axis; zero layer. (c) Rotation the same as (b); first layer. (d) The composite reciprocal lattice reconstructed. († indicates that the angle is measurable only approximately on this diagram.)

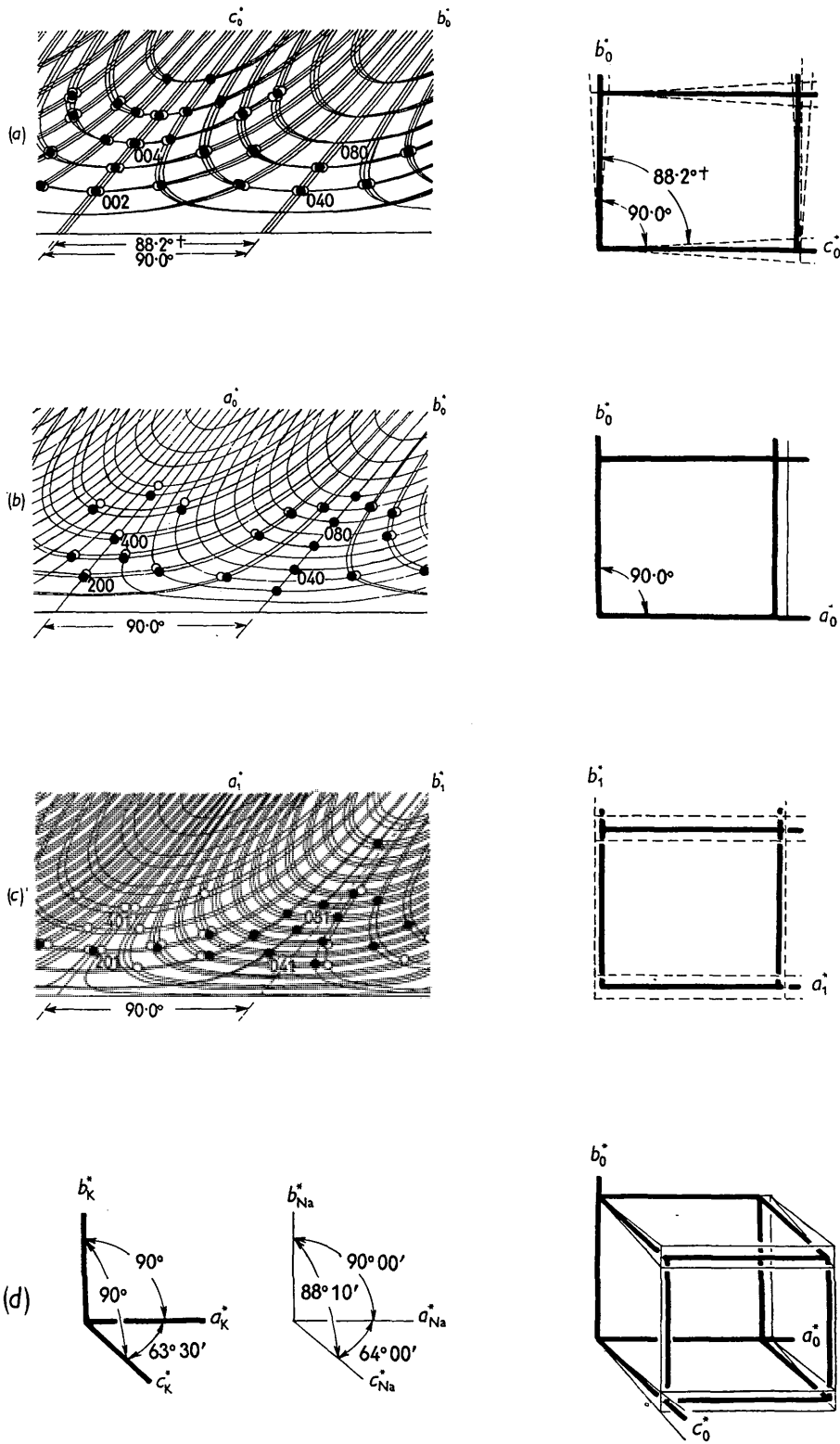


Fig. 3. Weissenberg diagrams of anorthoclase (core part), showing that it is composed of three crystals, one being monoclinic potassium felspar and the remaining two triclinic albite- and pericline-twinned sodium felspars. Notation as in Fig. 1. (a) Rotation about the  $a$  (monoclinic) axis; zero layer. (b) Rotation about the  $c$  (monoclinic and triclinic) axis; zero layer. (c) Rotation the same as (b); first layer. (d) Reciprocal lattices (monoclinic and triclinic albite-twinned) reconstructed. ( $\dagger$  indicates that the angle is measurable only approximately on this diagram.)

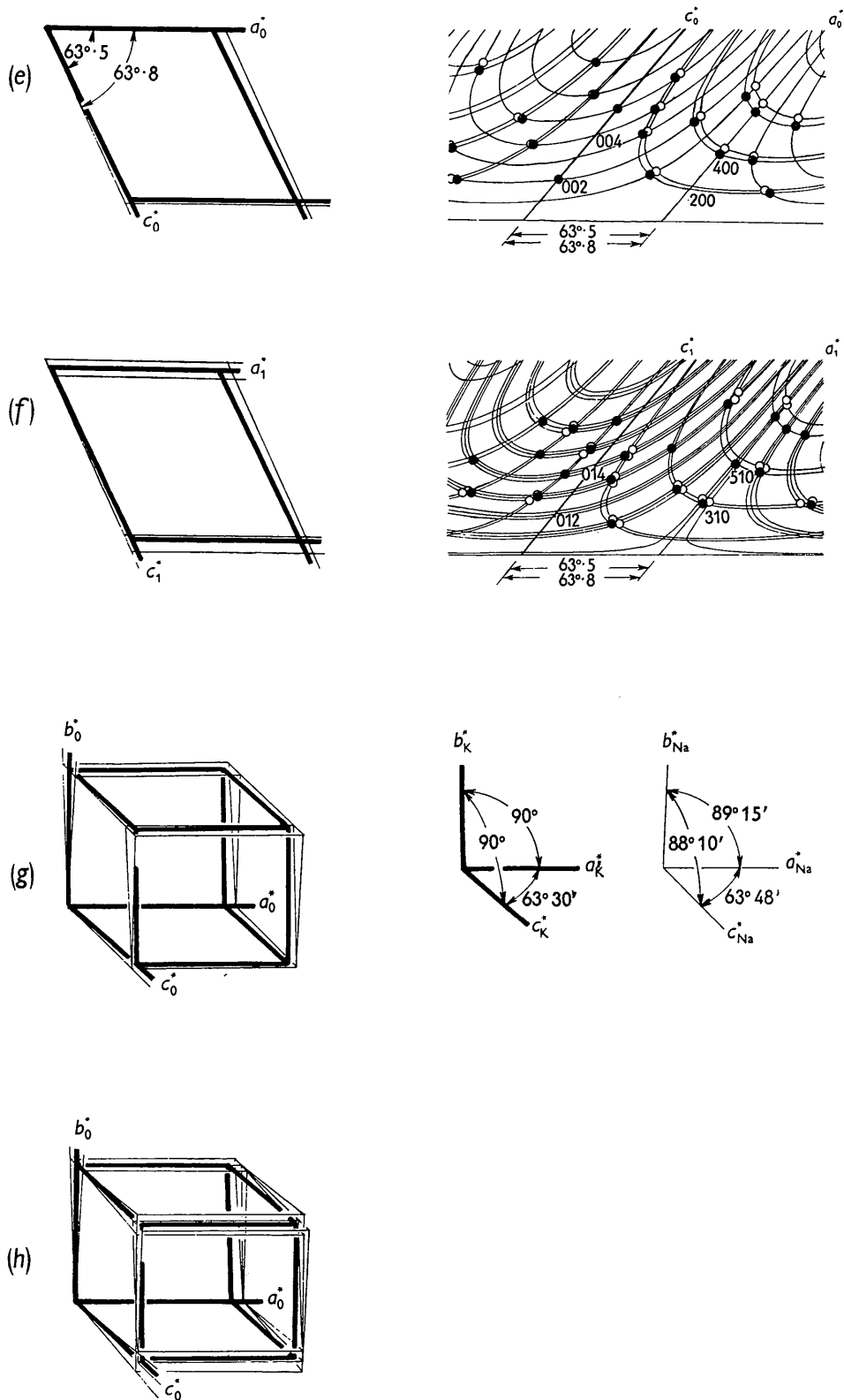


Fig. 3 (cont.). (e) Rotation about the  $b$  (monoclinic and triclinic) axis; zero layer. (f) Rotation the same as (e); first layer. (g) Reciprocal lattices (monoclinic and triclinic pericline-twinned) reconstructed. (h) The composite reciprocal lattice reconstructed.

cut from the rim (analysis (2)) and core (analysis (3)) of the composite crystal (Figs. 2 and 3). The preliminary examinations by the rotation photographs revealed that there exists, forming the major part of it, a monoclinic component both in the rim and core. Fig. 2(a), taken with the monoclinic  $a$  axis as the rotation axis, shows further that a triclinic feldspar accompanies the monoclinic one. The former is twinned after the albite law, as evidenced by the symmetrical branching of  $[001]^*$  of it against that of the latter,  $[010]^*$  coinciding. This may be confirmed by the  $c(0)$  and  $c(1)$  Weissenberg diagrams reproduced in Fig. 2(b) and (c). In these diagrams, as illustrated by the attached reciprocal-net planes, the triclinic  $[100]^*$  lines on the first or higher level are ramified, whereas they are simple on the zero level. Of course,  $[010]^*$  lines on all levels are single, as should be the case in albite twins.

In the core part an  $a(0)$  Weissenberg diagram (Fig. 3(a)) reveals immediately that we have here to deal with the pericline- as well as albite-twinned feldspars as the counterpart products of the monoclinic feldspar, as testified by the branching of both  $[010]^*$  and  $[001]^*$ . While albite twinning, exactly as in the rim part, gives rise to the pairing of  $[100]^*$  on the  $c(1)$  or higher, Weissenberg diagrams (Fig. 3(b) and (c)), but not on the  $c(0)$  diagram, pericline twinning is demonstrated by the  $b$  (monoclinic) Weissenberg diagrams (Fig. 3(e) and (f)), which show that doubling of  $[100]^*$  occurs on the first, and not on the zero, level,  $[001]^*$  remaining always single on all levels.†

The direct-lattice and reciprocal-lattice constants of each constituent feldspar were deduced, taking into account the fact that some of the net planes are not on the same level and appear on the same Weissenberg

†  $c_1^*$ ,  $c_2^*$  etc. are not split, since  $(b_0^* c_0^*)$  and  $(b c_0^*)$  planes coincide because  $\gamma = b \wedge a = 90^\circ$  (specially for this feldspar) and  $b_0^* \wedge a = 90^\circ$ ,  $c_0^* \wedge a = 90^\circ$  (by definition) (Fig. 4).

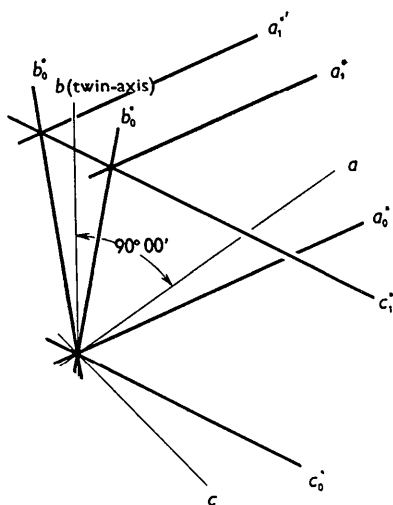


Fig. 4. Illustration of the non-splitting of  $[001]^*$  in the pericline-twinned feldspar when  $\gamma$  is  $90^\circ$ .

photograph because of the tolerance of the slit (Table 2(b)).

From these we have deduced that there exist in anorthoclase two (rim part) or three (core part) different feldspars growing side by side. One of them is potash-rich and monoclinic and the remaining soda-rich and triclinic. The soda feldspars are twinned either after the albite or pericline law. In the albite-twinned soda feldspar (100) and  $[001]$ , and in the pericline-twinned one (100) and  $[010]$ , are respectively parallel to those of the associated monoclinic (potash) feldspar. The (100) planes are left unchanged in orientation by pericline twinning while they are brought to the parallel positions by albite twinning, as already mentioned, on account of particular value of  $\gamma^*$ , namely  $90^\circ$ , a relationship which seems to be maintained in the feldspars of this kind.

It is further to be noted the monoclinic and albite-twinned triclinic components of the rim and core parts are respectively of the same composition, with lattice constants identical within the experimental errors.

From the intensity measurements on the Weissenberg photographs it may be concluded that the rim part of anorthoclase is composed of 71% potash feldspar and 29% albite-twinned soda feldspar, and the core of 50% potash feldspar, 21% albite-twinned soda feldspar and 29% pericline-twinned soda feldspar. These correspond respectively to the ratios of 74:26 and 49:51 of the potash and soda contents of anorthoclase parts, as revealed by chemical analyses. However, how the small lime content is distributed over the component feldspars and the potash and soda contents are exchanged isomorphously among them is unknown owing to the lack of exact informations as to the relationship between the lattice constants and chemical compositions of feldspars.

#### 4. On chemical compositions, lattice angles and twinning

Including moonstone, of which we reproduce in Table 2(c) the data given in the previous account (Ito, 1950), we have now examined a number of feldspars of the potash-soda series covering a fairly wide range of composition. They are all exsolution products on either a microscopic or submicroscopic scale, being composed of the soda- and potash-rich constituents. Summarizing these results, as given in Table 3, we find that the albite-twinned soda feldspar is the sole companion of the potash feldspar when the latter is predominating (70% or more). If the potash feldspar is less than 70% the pericline-twinned soda feldspar appears in addition to the albite-twinned one, and this takes place in such a fashion that the ratio of the latter to former decreases as the preponderance of the potash feldspar over soda feldspar diminishes. When the percentage of the potash feldspar becomes as low as 40%, against 60% of the associated soda feldspar, the albite-twinned soda feldspar disappears entirely leaving the pericline-twinned, sometimes together with the monoclinic,



Table 3. Constitution of the potash-soda feldspars

	Anorthoclase			
	Microcline	Rim	Core	Moonstone
Percentage of the constituent feldspars as determined by the X-ray method	I'. K-rich 82 %	I''. K-rich 71 %	I'''. K-rich 50 %	I'''. K-rich 42 %
	II'. Na-rich 18 %	II''. Na-rich 29 %	II''. Na-rich 21 %	II'''—V'''. Na-rich 58 %
			III'''. Na-rich 29 %	
Ratio of Or- to Ab-molecules as calculated from chemical analysis	77 : 23	74 : 26	49 : 51	41 : 59
Twinning of the constituent feldspars	Albite (II')	Albite (II'')	Albite (II'') Pericline (III'')	Pericline (III'''—V''')

soda feldspars as the only counterpart products of the potash feldspar in the process of exsolution.

It is interesting to note that in the pericline-twinning feldspars the (direct)  $\gamma$  angle and in the albite-twinning feldspars the (reciprocal)  $\gamma^*$  angle have persistently been found to be  $90^\circ$ , irrespective of the nature of the mother feldspar—microcline, anorthoclase or moonstone—from which they have been produced upon exsolution. This is natural, for pericline twinning has the (direct)  $b$  axis and albite twinning the (reciprocal)  $b^*$  axis as the twin axis. The ease with which polysymmetric synthesis takes place in a triclinic crystal when one of its direct zone angles is  $90^\circ$  has already been instanced in the wollastonite group of minerals (Ito, 1950, p. 101). The foregoing examples have shown that a similar statement is applicable to the reciprocal angles.

### References

- BÖGGILD, O. B. (1911). *Z. Krystallogr.* **48**, 466.  
 BUERGER, M. J. (1937). *Amer. Min.* **22**, 416.  
 CHAO, S. H. & TAYLOR, W. H. (1940). *Proc. Roy. Soc. A*, **174**, 57.  
 HADDING, A. (1921). *Acta Univ. Lund*, **2**, 17.  
 ITO, T. (1935). *Beitr. Min. Japan*, N.F. No. 1.  
 ITO, T. (1938). *Z. Krystallogr.* **100**, 297.  
 ITO, T. (1950). *X-ray Studies on Polymorphism*. Tokyo: Maruzen.  
 KÔZU, S. & ENDÔ, Y. (1921). *Sci. Rep. Tôhoku Univ.*, series 3, **1**, 1.  
 KÔZU, S. & SUZUKI, M. (1921). *Sci. Rep. Tôhoku Univ.*, series 3, **1**, 19.  
 LANGE, J. J. DE, ROBERTSON, J. M. & WOODWARD, I. (1939). *Proc. Roy. Soc. A*, **171**, 398.  
 LAVES, F. (1950). *J. Geol.* **58**, 551.

*Acta Cryst.* (1952). **5**, 449

## Compounds of Thorium with Transition Metals.

### I. The Thorium-Manganese System\*

BY JOHN V. FLORIO, R. E. RUNDLE AND A. I. SNOW†

*Institute for Atomic Research and Department of Chemistry, Iowa State College, Ames, Iowa, U.S.A.*

(Received 16 November 1951)

Like uranium, thorium forms no compounds with chromium, a few with manganese, the number increasing through nickel, and decreasing sharply with copper. The structures of the compounds of thorium with manganese, reported in detail here, are unlike those with iron, cobalt and nickel, which are generally similar.

$\text{ThMn}_2$  has the  $\text{MgZn}_2$  (C14-type) structure;  $\text{Th}_6\text{Mn}_{23}$  is face-centered cubic with a unique structure; while  $\text{ThMn}_{12}$  is body-centered tetragonal with a structure similar to, but not identical with, the corresponding iron, cobalt and nickel compounds.

### Introduction

The compounds of thorium with the transition elements of the first period are particularly numerous and interesting, and display several new structural types. The present empirical stage in the development of theories of intermetallic-compound formation suggests that further structural studies will be im-

portant aids to progress in this field. We have, therefore, undertaken a systematic study of the structures

\* Contribution No. 189 from the Institute for Atomic Research and Department of Chemistry, Iowa State College, Ames, Iowa. Work performed in the Ames Laboratory of the Atomic Energy Commission.

† Present address: Institute for the Study of Metals, University of Chicago, Chicago, Illinois, U.S.A.